R. & M. No. 2779
(13,436, 14,695)
A.R.C. Technical Report

MINISTRY OF SUPPLY

AERONAUTICAL RESEARCH COUNCIL
REPORTS AND MEMORANDA

PART I

The Effect on Transition of Isolated Surface Excrescences in the Boundary Layer

By
N. GREGORY, M.A., and W. S. WALKER,
of the Aerodynamics Division, N.P.L.

PART II

Brief Flight Tests on a *Vampire I* Aircraft to Determine the Effect of Isolated Surface Pimples on Transition

By
D. JOHNSON,
of the Royal Aircraft Establishment

LONDON: HER MAJESTY'S STATIONERY OFFICE
1956
PRICE 6*s* 6*d* NET

PART I

The Effect on Transition of Isolated Surface Excrescences in the Boundary Layer

By

N. GREGORY, M.A., and W. S. WALKER,
of the Aerodynamics Division, N.P.L.

PART II

Brief Flight Tests on a *Vampire I* Aircraft* to Determine the Effect of Isolated Surface Pimples on Transition

By

D. JOHNSON,
of the Royal Aircraft Establishment

Reports and Memoranda No. 2779
October, 1951

PART I

The Effect on Transition of Isolated Surface Excrescences in the Boundary Layer

Summary.—The effect of isolated surface excrescences in a laminar boundary layer in producing disturbances which may lead to turbulent flow has been examined experimentally by several methods. Photographs of some of the flow patterns visualised by smoke and china-clay techniques are given.

The critical heights of pimple which just give rise to spreading wedges of turbulent flow have been measured on a flat plate and on two aerofoils at several angles of incidence. The results are analysed and are presented in a form which enables approximate estimates to be made of the protuberances permissible on laminar-flow surfaces at full-scale flight Reynolds numbers. The estimates suggest that at an altitude of 30,000 ft the critical pimple height is 0·004 in. for a speed of 350 m.p.h., whilst 0·002 in. may be permissible at all subsonic speeds. At sea-level, however, the tolerances are approximately halved.

1. *Introduction.*—Advances in aerodynamic design during the last decade have led to the conception of aerofoils and bodies designed and constructed for considerable extents of laminar flow. In theory this may be achieved by producing a favourable velocity gradient (increasing velocity) from the front stagnation point for as far as possible. But laminar flow and low drag will not be realised unless the surface is 'aerodynamically' smooth. Fage (R. & M. 2120[1], 1943) has shown that small spanwise ridges or protuberances can cause transition to take place with

Part I published with the permission of the Director, National Physical Laboratory.
Part II (R.A.E. Tech. Memo. Aero. 210, received 3rd March, 1952) communicated by the Principal Director of Scientific Research (Air), Ministry of Supply.

consequent increase in drag. The effect of small isolated excrescences is nearly as great, for if transition takes place, the turbulent flow downstream of each protuberance spreads spanwise in the form of a wedge, contaminating large areas of the surface. Summarising past experiments Richards[2] (1950) shows that an aircraft whose wing was studded with large rivets had its top speed reduced by 7 per cent. On a transport aircraft with a laminar-flow wing a more severe restriction in pay-load or range would result.

It is useful to know the maximum size of protuberance on a wing that can be tolerated without affecting the transition position. Fage (R. & M. 2120[1]) has investigated this for two-dimensional ridges, hollows and wires. The present paper deals with the similar problem for isolated three-dimensional excrescences, or 'pimples'.

The flow observed past the pimples is described in sections 3 and 4. In addition, standard shapes of pimples were attached to several aerofoil surfaces; the measurements made are given and analysed in sections 5 and 6. The practical application is discussed in section 7.

2. *Pimple Shapes.*—In past experiments with isolated roughnesses, such as those performed with rivet heads by Hood[3] (1939), the drag increment was divided into two parts, the form drag of the pimple itself, and the extra drag if laminar flow was replaced by a wedge of turbulent flow. With natural transition well forward, the form drag of the pimple was generally the most important part. But for laminar-flow aerofoils with far-back transition, it is the drag increment due to the wedge of turbulent flow that is significant. The shape of pimple is important therefore, only in so far as it affects the size of pimple that first gives rise to turbulent flow. This effect can be avoided by making different sized pimples of constant geometrical proportions.

A reproducible pimple was first produced in the present series of experiments by inserting a short length of fine wire into an aerofoil surface and filing it flush with a thickness template drilled to fit over the wire. Wires 0·007, 0·010, 0·012, 0·015 and 0·020-in. in diameter were used, and the pimple heights were made equal to the diameters.

An adjustable pimple was subsequently used, consisting of a 60-deg cone, turned on the end of a fine-pitch screw. The space between the pimple and the threaded socket in the surface was carefully plugged with Plasticene and smoothed. The height of pimple protruding was measured with a dial gauge.

Some additional tests were performed with adjustable cylindrical pimples of squat proportions. Two diameters, 0·1 and 0·2 in. were used in conjunction with pimple heights of 0·006 to 0·100 in. These pimples may be likened to imperfectly fitted flush rivets.

3. *Visualisation of Transition by China-clay and Smoke Techniques.*—Cylindrical and conical pimples were screwed into a flat plate which had been coated with china-clay lacquer. Oil of wintergreen (methyl salicylate) was used as the indicating liquid. Figs. 1 and 2 show the patterns that were obtained at a wind speed of 120 ft/sec with various heights of pimple. At the smallest heights, two white streaks are seen spaced about a pimple diameter apart. With the conical pimple, one line only is visible: it is likely that both are present, but that they cannot be resolved. As the pimple height is increased, a wedge of turbulent flow appears, and the point of breakdown of the laminar flow gradually approaches the pimple over a range of pimple height. It is shown later that this is peculiar to the flat plate; on two aerofoils the smallest possible increase in pimple height (0·001 in.) encompassed the change from twin streaks to a fully turbulent wedge emanating from the pimple.

The last picture in Fig. 1 was obtained with a 0·1-in. high pimple glued on to the plate. This avoided the absorbent Plasticene packing and shows that the area of dried-out china clay, or high surface-shear, extends round the front of the pimple.

The flow at the front of the pimple was examined on a larger physical scale in a low-speed smoke tunnel. The pimples were chosen about $\frac{3}{4}$-in. high in a boundary layer slightly thicker than this, and the wind speed was about 4 ft/sec so that the Reynolds number based on the pimple height and velocity at the tip of the pimple remained unchanged. Paraffin smoke was

emitted from holes in a very fine streamlined strut placed upstream of the pimple. Pictures of the smoke flow round various sections of the pimple are shown in Fig. 3. The boundary layer produces a static-pressure gradient along the front stagnation generator of the cylinder. There is consequently an inflow towards the plate and a reverse flow forwards along its surface. The fluid rolls up into a number of continuously generated horseshoe-shaped vortices which are seen wrapped round the cylinder and trailing downstream as a multi-ply vortex pair with axes parallel to the direction of the main flow. The number of vortices in front of the pimple, all rotating in the same direction, depends on the speed of the flow; as many as three have been observed. In Fig. 3(c) there are two vortices, but in the orthogonal view below, only the inner vortex is fed with smoke and made visible.

The vortex pattern of flow has been observed with smoke over a wide range of conditions. Stream speeds up to 16 ft/sec (the maximum for the tunnel) with pimples ranging in height from 0·06 in. to 1 in. in boundary layers slightly thicker than the pimples have all yielded vortices. The pimple shape has little effect. Vortices were observed with conical pimples of 60-deg cone angle and even with an irregular mound of Plasticene* with a maximum slope of 25 deg.

4. *Flow behind the Pimple.*—4.1. *Regular Pattern in the Wedge of Turbulent Flow.*—During the experiments with pimples on the flat plate at the minimum speed of test (40 ft/sec) when the pimple was set at the critical height, the china-clay record of the wedge of turbulent flow revealed a fine structure, Fig. 4. After prolonged exposure to the air stream, the china-clay picture was indistinguishable from those obtained at higher speeds. Similar flow patterns behind a pimple were observed in the low-speed tunnel with wind speeds up to 16 ft/sec. The china-clay technique was adapted to these speeds by using amyl acetate as an indicator; although the lacquer was softened temporarily, no adverse effects ensued. Fig. 5 shows that the patterns obtained in the smoke tunnel with china-clay are confirmed by the pictures taken of thin sheets of smoke emitted from slits across the plate, in front of and behind the pimples.

The observations showed that the flow pattern and the manner of breakdown of the flow to turbulence changed with the Reynolds number of the experiment. At small Reynolds numbers, a pair of spiral smoke filaments were observed arising normally to the plate close behind the cylinder. On reaching the level of the top of the cylinder, the smoke filaments trailed downstream very close to each other along the centre-line. As the wind speed was increased, a spreading turbulent wake appeared downstream of the cylinder, exhibiting a fine structure; the spiral filaments remained undisturbed. At larger Reynolds numbers, the horseshoe-shaped vortex appeared, wrapped round the front of the cylinder. These were the conditions under which Fig. 5 was observed. A diagrammatic explanation of Fig. 5c and 5d is given in Fig. 6, which suggests that dissipating plumes of smoke indicate flow away from the surface, and hence the rising edges of vortices in the boundary layer. At still larger Reynolds numbers, the twin vortex filaments leaving the top of the cylinder break down, and eddies are shed. In this case, there is no central plume of smoke from the second slit, and the horseshoe vortex is the most prominent feature of the flow.

An attempt was made to measure the frequencies with which the eddies were shed from the top of the pimple by observing the smoke stroboscopically. Precise measurements were not obtained, owing to unsteadiness in the flow and rapid diffusion of the smoke. Owing to the scatter of the results, it is difficult to say whether the non-dimensional frequency parameter $f\varepsilon/u_\varepsilon$ (where f is the frequency, u_ε the velocity at the top of the pimple of height ε) is a function of R_ε $(= u_\varepsilon\,\varepsilon/\nu)$ alone. For pimples nearly as thick as the boundary layer, $f\varepsilon/u_\varepsilon$ increases roughly from 0·2 to 0·3 as R_ε increases from 600 to 1,300. Above $R_\varepsilon = 1{,}300$ it is possible, but not certain, that $f\varepsilon/u_\varepsilon$ becomes constant and equal to 0·4. Reliable observations of this particular phenomenon could more easily be obtained in a water-tunnel where the whole field of flow can be made visible instead of a few isolated stream filaments.

* The vortex in this case corresponds to the windward eddy observed by meteorologists in front of an isolated hill.

The reason for the fine structure observed with smoke and china-clay remains uncertain. The evidence points to a duplication and reduplication of the original vortex pair which was generated in front of the cylinder, thus creating a system which decays further downstream of the cylinder to true turbulence. The boundary layer may possibly become unstable in the presence of the finite vortex pair, though it is not unstable to infinitesimal vortex disturbances by reason of any centrifugal or temperature effects. The latter instabilities have already been thoroughly investigated; as the experimental phenomena they produce are similar to those of the present experiments, the work on these dynamic instabilities of the laminar boundary is briefly reviewed below.

The criterion for instability of a layer of fluid confined between two walls when a temperature gradient exists across the fluid has been obtained mathematically by Rayleigh[4] (1916), for stationary fluid and by Low[5] (1929) for shear flow. The convective circulation of the unstable fluid has been observed experimentally by Bénard and Avsec[6] (1938) and also by Chandra[7] (1938) who have shown that when one of the walls is in motion, giving a shear flow, the circulation pattern becomes alternating rows of vortices with axes lying along the direction of the flow. Smoke pictures of the vortices, similar to the present pictures were obtained. The temperature difference necessary between the two walls is 20 deg C for a layer 1-cm thick, the difference increasing for narrower layers. Chandra observed a slightly different smoke pattern which appears in thin layers for very much smaller temperature differences.

The production of rows of vortices under the influence of centrifugal effects has been investigated both theoretically and experimentally for the flow between co-axial circular cylinders by Taylor[8] (1923) and theoretically for boundary-layer flow on a concave surface by Görtler[9] (1941) Direct evidence of the Görtler-type vortices is given in Fig. 7, a photograph taken in the National Physical Laboratory 13 × 9-ft Wind Tunnel of the china-clay representation of flow past the 30 per cent thick Griffith aerofoil with a high rate of suction at the slot. A fresh laminar boundary layer starts on the concave surface of the flap and the china-clay streaks indicate the Görtler vortices. They compare with the present china-clay pictures. The streaks in Fig. 7 resemble those of Figs. 4 and 5 and may possibly arise in a similar manner, but this suggestion needs theoretical investigation.

4.2. *Angle of Spread of Turbulent Flow.*—The photographic records of wedges of turbulent flow observed by the china-clay technique on several aerofoils in the N.P.L. 13 × 9-ft Wind Tunnel have been examined, and the angle of spread of the wakes measured. The results are given in the accompanying Table 1. In some cases the edges of the wakes are straight, in others the angle of spread increases further downstream from the pimple.

TABLE 1

Aerofoil	Chord (in.)	Tunnel wind speed (ft/sec)	Wedge angle (deg)	Remarks
Flat plate	18	30 60	7 to 14	Conical pimples near critical height Angle increases from apex towards trailing edge
Flat plate	18	120	16	Cylindrical and conical pimples at all heights
30% Griffith	30	180	15	From 0·1 to 0·7 chord
NACA 66_2-015	48	180	17	From leading edge to 0·7 chord
13% section	60	180	8 to 12 12 to 16½	From pimple 0·05c to 0·2c From 0·2c to 0·6c
NACA 65_3-018	72	180	18½	From leading edge to 0·7 chord

These latter are probably cases in which the pimple is set close to the critical height. The aerofoils tested were all at 0-deg incidence with moderately favourable pressure gradients. It is suggested that the observed variation in wedge angle between 14 deg and 8 deg may be associated with changes in Reynolds number as well as changes in pressure gradient.

5. *Observations of the Critical Pimple Height.*—The critical pimple heights at which wedges of turbulent flow first formed were found, with the aid of the china-clay technique described in section 3, for various shaped pimples on different aerofoil sections. The experiments were performed in the N.P.L. 13 × 9-ft Wind Tunnel and details of the five sets of observations are given in Table 2. In the case of the 15 per cent Roof-top Section, the pimple heights were fixed and the tunnel-wind speed was adjusted until the spreading turbulent wedge occurred. For all the other tests the normal procedure was followed of choosing the wind speed and then adjusting the pimple height until transition occurred.

TABLE 2

Aerofoil	Chord (in.)	Incd. (deg)	Pimple shapes	Range of tests
15% Roof-top	30	0	Cylindrical, height = diameter	8 chordwise positions 5 pimple heights, variable speed
13% section	60	−8	Conical	9 chordwise positions Wind speed from 30 to 180 ft/sec; variable pimple height
,,	,,	0	,,	,, ,, ,,
,,	,,	2	,,	,, ,, ,, with extra positions at 40 and 60 ft/sec
Flat plate	18	0	Conical, and squat cylindrical 0·1 and 0·2-in. dia.	3 chordwise positions, speed range 40 to 180 ft/sec

The aerofoils concerned have been previously reported on; the 15 per cent Roof-top Section (N.P.L. 150)[10] by Cheers, Walker and Taylor (R. & M. 2412, 1946[11]) and the 13 per cent low-drag section* (N.P.L. 335)[10] by Cumming, Gregory and Walker (R. & M. 2742, 1950[12]). The experimental velocity distributions on the working surfaces of the two aerofoils are given in Fig. 8, and the numerical observations are presented graphically in Figs. 9 to 12. The curves show that there is a chordwise position on the surface of an aerofoil where the critical pimple height is a minimum. At the stagnation point itself, an indefinitely large pimple would presumably be permissible. The observations of Fig. 11 have been cross-plotted in Fig. 13 so as to emphasize the variations of critical pimple height with wind speed.

It was found that a change of one or two thousandths of an inch in the height of a pimple on the aerofoils encompassed the change from the decay of a horshoe vortex to the spread of a wedge of a fully turbulent flow with apex at the pimple. The height of pimple at which this change occurred was taken as the critical height. With the flat plate, however, the appearance of the turbulent wedge was spread over such a considerable range of pimple heights that the whole range had to be described as 'critical'. These latter results possessed so much scatter that smooth curves could not be drawn with any confidence. The observations are therefore not given here in detail, but are commented on later.

Some additional results with zero pressure gradient were obtained on the 13 per cent section at 40 and 60 ft/sec at an incidence of + 2 deg, corresponding to constant surface velocity as on the flat plate. The wedge of turbulence still appeared suddenly, as the pimple height was

* The present tests were performed on the surface without the slot.

increased. Yet there was considerably more scatter than with favourable gradients, and this could not be correlated with waves in the pressure distribution or with ripples in the surface. Taken together with the observations on the flat plate at zero incidence, these results show that in the absence of favourable pressure gradient the critical pimple height is highly sensitive to changes in external conditions, and that absence of surface curvature causes the effects to be spread out over a range of pimple height and distance along the surface.

6. *Analysis of the Numerical Observations of Critical Conditions.*—In this section the various factors which are likely to affect the critical height of pimple just causing a spreading wedge of turbulent flow are considered. An empirical relation which fits the experimental data is suggested as a basis for extrapolation.

6.1. *Notation.*

ε Critical pimple height

d Diameter of the base of the pimple

δ^* Displacement thickness, a convenient measure of the boundary-layer thickness

s Distance from the front stagnation point

U Velocity at the edge of the boundary layer

u_ε Velocity at the tip of the pimple

$\chi = \frac{s}{U}\frac{dU}{ds}$

ρ Density of the fluid

μ Viscosity of the fluid

$\nu = \mu/\rho$

τ_0 Shearing stress at the surface

$R_s = \frac{sU}{\nu}$, Reynolds number based on distance from stagnation point and local velocity outside layer

$R_\varepsilon = \frac{\varepsilon u_\varepsilon}{\nu}$, Reynolds number based on height of pimple and velocity at tip of pimple

$\phi = \frac{\tau_0}{\rho U^2} R_s^{1/2}$, non-dimensional function representative of the surface friction

$\bar{\delta} = \frac{\delta^*}{s} R_s^{1/2}$, non-dimensional function representative of the boundary-layer thickness

$\bar{\varepsilon} = \frac{\varepsilon}{s} R_s^{1/2}$, non-dimensional function representative of the pimple height

6.2. *The Analysis.*—The values of U, δ^*, ρ, μ, τ_0, s and dU/ds at the position of the pimple determine both the local and the overall field of flow and therefore may affect the critical height of pimple. The pimple shape is also of importance; it is difficult to specify this completely by a limited set of numerical factors, but for standard shapes of pimples, such as cylinders and cones, the diameter of the base of the pimple, d, can be considered to be a second parameter which should be included.

Other factors, the effect of whose variation is less certain, are the curvature of the surface and the turbulence of the flow. They will not be considered further at the moment.

The application of dimensional analysis (*e.g.*, Buckingham[13], 1914) enables the functional relationship between the critical pimple height and the factors enumerated above to be written in the form

$$f_1\left(\frac{\varepsilon}{s}, \frac{\delta^*}{s}, \frac{d}{s}, R_s, \chi, \frac{\tau_0}{\rho U^2}\right) = 0 . \quad .. \quad .. \quad .. \quad .. \quad .. \quad .. \quad .. \quad (1)$$

In this relation, any term may be replaced by any combination of it and others. Now by definition

$$R_\varepsilon = \frac{\varepsilon u_\varepsilon}{\nu} = \frac{\varepsilon}{s}\frac{u_\varepsilon}{U} R_s = \bar{\varepsilon}\frac{u_\varepsilon}{U} R_s^{1/2} , \quad .. \quad .. \quad .. \quad .. \quad .. \quad .. \quad .. \quad (2)$$

and if the laminar boundary-layer velocity profiles are assumed to form a one-parameter family, the profile is fixed by the value of ϕ so that u_ε/U is a function of ϕ and $\bar{\varepsilon}$ only. Therefore R_ε is a function of $\bar{\varepsilon}$, ϕ and R_s only. Thus equation (1) may be written

$$R_\varepsilon = f_2\left(\bar{\varepsilon}, \bar{\delta}, \frac{d}{\varepsilon}, \chi, \phi\right) . \quad .. \quad .. \quad .. \quad .. \quad .. \quad .. \quad .. \quad (3)$$

At each chordwise position, χ, ϕ and $\bar{\delta}$ remain constant while the pimple height is varied, and the ratio d/ε is a constant for conical shaped pimples. Fig 14 shows how R_ε varies with $\bar{\varepsilon}$ for various chordwise pimple positions on the 13 per cent section at zero incidence*: the greater the pimple height relative to the boundary-layer thickness, the greater the value of R_ε. It was noticed that the curves are all similar in shape, and it was found that they could be reduced to a single curve, Fig. 15, when the values of R_ε on each curve are divided by the appropriate ordinate R_ε for the station $\bar{\varepsilon}$ equal to one. Moreover, it was found that the same curve of $R_\varepsilon/(R_\varepsilon)_1$ [where suffix 1 refers in general to the station $\bar{\varepsilon} = 1$] as a function of $\bar{\varepsilon}$ was obtained at the other incidences at which tests where carried out. A result in this form (R_ε as a function of $\bar{\varepsilon}$) is inconvenient for practical application as the unknown ε occurs on both sides of the relation.

However, it is suggested by Figs. 14 and 15 that, for values of $\bar{\varepsilon}$ less than 1·5,

$$R_\varepsilon\left(\equiv \bar{\varepsilon} \cdot \frac{u_\varepsilon}{U} R_s^{1/2}\right) = \bar{\varepsilon}(R_\varepsilon)_1 . \quad .. \quad .. \quad .. \quad .. \quad .. \quad .. \quad (4)$$

For these values of ε, the boundary-layer profile may also be assumed linear so that

$$u_\varepsilon/U = \bar{\varepsilon}(u_\varepsilon/U)_1 \text{ approximately.} \quad .. \quad .. \quad .. \quad .. \quad (5)$$

Hence, dividing

$$\frac{R_\varepsilon}{u_\varepsilon/U}\left(\equiv \bar{\varepsilon} R_s^{1/2}\right) = \left[\frac{R_\varepsilon}{u_\varepsilon/U}\right]_1 \text{ approximately.} \quad .. \quad .. \quad .. \quad .. \quad (6)$$

The function $[R_\varepsilon/(u_\varepsilon/U)]_1$ or $[\varepsilon U/\nu]_1$ will be denoted by F, and it should be noted that $\varepsilon U/\nu$ is approximately constant at any given pimple position for all pimples within the linear portion of the boundary-layer velocity-profile. Within this region, equation (6) gives us

$$\frac{\bar{\varepsilon}}{F} = R_s^{-1/2} . \quad .. \quad .. \quad .. \quad .. \quad .. \quad .. \quad .. \quad (7)$$

This deduction from equations (4) and (5) has also been noted by Keeble and Atkins[14] (1951).

The experimentally derived values of $\bar{\varepsilon}/F$ together with curves of $R_s^{-1/2}$ are plotted against R_s for all values of ε in Figs. 16 to 19 for all four aerofoil cases tested, and the values of F at each pimple position are plotted against s/c in Fig. 20. Despite the variations in boundary-layer

* In order to obtain u_ε/U from the experimental values of the pimple height, the theoretical boundary-layer thickness has been assumed to be that obtained by Falkner's simplified method (R. & M. 1895) and the appropriate velocity profile has been taken. Two checks showed that this method gives velocities within 10 per cent of those measured in an experimental boundary-layer traverse.

velocity-profile shape from test to test, and the use of values of ε extending beyond the limits within which the approximations of equations (4) to (7) hold, it appears from Figs. 16 to 19 that a single relation between $\bar{\varepsilon}/F$ and R_s is obtained. This result is given by equation (7) when R_s is greater than about 3×10^5; below this Reynolds number the pimple height exceeds the distance over which the boundary-layer velocity-profile remains linear. Thus this universal curve, together with the various relations between F and s/c of Fig. 20 neatly summarize all the experimental data.

That the above empirical analysis is not inconsistent with the dimensional analysis may be shown by writing equation (1) in the following form

$$\bar{\varepsilon} = \mathrm{f}_3 (R_s, \chi, \phi, \bar{\delta}, d/\varepsilon) . \qquad (8)$$

If it is assumed that the scale effect may be separated from the others as is suggested by the similarity of the experimental curves of Fig. 14, then equation (8) may be written

$$\bar{\varepsilon} = \mathrm{f}_4 (R_s)\ \mathrm{f}_5 (\chi, \phi, \bar{\delta}) \qquad (9)$$

where the parameter d/ε has been dropped since attention is being confined to the conical shaped pimples.

The empirical result of Figs. 16 to 19, namely that $\bar{\varepsilon}/F$ is a universal function of R_s suggests that F may perhaps be identified with $\mathrm{f}_5 (\chi, \phi, \bar{\delta})$.

The observations on the 15 per cent Roof-top aerofoil, where the pimples were cylinders of height equal to diameter instead of cones, have been plotted in Figs. 19 and 20 with the rest. It is evident that the different pimple shape has not affected the results and this suggests that for the values of d/ε close to unity, the precise pimple shape may be disregarded.

The suggested variation of F with precise changes in χ, ϕ and $\bar{\delta}$ for the four tests has not been investigated owing to the small amount of data available, but some similarity will be evident between the curve of F against s/c (Fig. 20) and the velocity distributions of Fig. 8. For the 13 per cent section at + 2 per cent incidence, f_5 would have been expected to be a constant over a considerable portion of the surface, since from 0·10-chord onwards, the velocity is nearly constant, and χ, ϕ, and $\bar{\delta}$ all rapidly approach constant values. It is possible that the variation in F is due to some parameter which has not been taken into account, such as curvature of surface.

This analysis was applied to the results from the flat plate, and for conical pimples it suggested that F should take roughly the values of 790, 910 and 1010 at positions $4\frac{1}{2}$, 9 and $13\frac{1}{2}$ in. from the leading edge of the plate, which was of 18-in. chord. If these figures are compared with those obtained on the 13 per cent section at + 2 deg incidence when the velocity gradient is also zero, on a basis of equal distances from the leading edge, the agreement is good.

The effect of the squat cylindrical pimples on the flat plate was observed in cases where the pimple height ranged from 0·012 in. to 0·050 in. It was found that the critical heights for the cylinders of 0·2-in. diameter were greater than the conical pimple heights by 0·003 in. or 0·004 in. and that those for the 0·1-in. diameter cylinders were greater than for the cones by 0·006 in. to 0·008 in.

Tunnel turbulence has not been considered in the analysis of the present experiments because tests on the flat plate were carried out in both the N.P.L. 13 × 9-ft and 4-ft Wind Tunnels at a wind speed of 60 ft/sec, and although the turbulence levels of the tunnels were greatly different no difference in the values of critical height was detected.

American Results.—Some similar work has been carried out in America by Loftin[15] (1946), the results from which have been grouped after the fashion of our equation (3). Loftin used cylindrical roughnesses of fixed diameter on two different aerofoils. He suggested that since ε was so small that the pimples were in that part of the boundary layer where u_ε/U was proportional to ε, then the local flow conditions would be similar in all cases, geometrical similarity would be

maintained, and hence R_ε for the critical conditions would be constant. In fact, Loftin found that as the Reynolds number of his experiment was increased, both ε and R_ε decreased. He ascribed this change in R_ε to the change in d/ε which was also present and he concluded by presenting a graph in which R_ε decreased, without much scatter of the experimental data, from a value of 900 when d/ε was 0·7 to 230 when d/ε was 4·5.

These conclusions are not confirmed by the present experiments which show, even for conical shaped pimples where d/ε is constant, an ordered decrease in R_ε as the Reynolds number is increased.

If the present method of analysis is applied to the American results, the values of $\bar{\varepsilon}/F$ fall close to the standard curve of Figs. 11 to 19, but the corresponding values of F are high, ranging from 825 to 0·06-chord to 2430 at 0·5-chord. The extreme height of the pimples is most noticeable in the experimental observations[15]; the reason remains a matter of speculation. It may be due to the very much lower turbulence level of the Langley low-turbulence tunnel. Or it may be associated with the different technique used, whereby the rise in profile drag due to a spanwise row of pimples was observed as the wind speed was increased. It is possible that isolated pimples actually gave turbulent wedges at much lower speeds than were detected.

7. *Practical Applications.*—The results may be used to predict critical values of the pimple height, for any given conditions, by means of the relation

$$\varepsilon = \frac{sF}{R_s^{1/2}}\left(\frac{\bar{\varepsilon}}{F}\right). \qquad (8)$$

$(\bar{\varepsilon}/F)$ is given by the universal curve shown in the graphs of Figs. 16 to 19, and the variation of F with s on the surfaces of two aerofoils at various incidences is given in Fig. 20. It is not expected that F will differ greatly for other aerofoils.

Above a Reynolds number (R_s) of about 3×10^5 the above equation simplifies to

$$\varepsilon = Fv/U \qquad (9)$$

and only Fig. 20 is needed.

The equation (8) has been used to calculate the critical pimple heights for the 13 per cent section at zero incidence at flight Reynolds numbers. The results are given for three sets of conditions in Table 3 together with a set of experimental observations at a lower Reynolds number.

TABLE 3

Case	1	2	3	4
Reynolds number based on chord R_c	$2{\cdot}9 \times 10^6$	$1{\cdot}4 \times 10^7$	$4{\cdot}8 \times 10^7$	$2{\cdot}2 \times 10^7$
Chord, ft	5	10	15	15
Speed ft/sec (at sea-level)	90	225	500	225
Speed ft/sec (at 30,000 ft)		500	(1,100)	500

Pimple position No.	Pimple position, s/c	Pimple height, thousandths of an inch			
1	0·008	19	4·6	1·8	4·4
2	0·017	16	4·0	1·7	3·9
3	0·025	14	4·2	1·8	4·1
4	0·05	12	4·8	2·3	5
5	0·075	14	5·8	2·6	5·8
6	0·100	15	6·5	2·9	6·2
		Experimental	Calculated		

The conditions for case 1, the experimental case, are representative of those applicable to very light aircraft, and sailplanes, and it should be quite easy to keep protuberances under 0·012 in. and achieve laminar flow, if the wing section has been correctly designed. In cases 2, 3 and 4 the low values of ε suggest that special precautions will be needed to obtain and maintain a smooth, clean and deposit-free surface. If this can be done, it should be possible to obtain laminar flow, at high altitude at least, right up to speeds where compressibility effects intervene.

8. *Conclusions.*—The numerical results suggest that at high altitudes the attainment of laminar flow with excrescences smaller than 0·004 in. may be possible up to air speeds as large as 350 m.p.h., whilst excrescences under 0·002 in. may always be permissible at subsonic speeds. At sea-level, however, the tolerances are smaller.

The investigation has yielded a considerable amount of information on the nature of the flow round an excrescence, and it has also brought to light a number of unexplained phenomena. In particular, the peculiar fine striations observed under certain conditions in the spreading wedge of turbulent flow behind a pimple are not fully understood. Further information on the frequency of the disturbances shed would be of interest and could be obtained more readily by means of tests in water than in air.

REFERENCES

No.	*Author*	*Title, etc.*
1	A. Fage	The smallest size of a spanwise surface corrugation which affects boundary-layer transition on an aerofoil. R. & M. 2120. 1943.
2	E. J. Richards	A review of aerodynamic cleanness. *J. R. Ae. Soc.*, Vol. 54, p. 137. March, 1950.
3	M. J. Hood	The effects of some common surface irregularities on wing drag. N.A.C.A. Tech. Note 695. 1939.
4	Rayleigh	On convection currents in a horizontal layer of fluid when the higher temperature is on the under side. *Phil. Mag.*, Vol. 32, p. 529. 1916.
5	A. R. Low	On the criterion for stability of a layer of viscous fluid heated from below. *Proc. Roy. Soc., A.*, Vol. 25, p. 180. 1929.
6	H. Bénard and D. Avsec ..	Travaux récents sur les tourbillons cellulaires et les tourbillons en bands. Applications à l'astrophysique et à la météorologie. *Journal de Physique et le Radium*, No. 11, p. 487. November, 1938.
7	K. Chandra	Instability of fluids heated from below. *Proc. Roy. Soc. A.*, Vol. 164, p. 231. 1938.
8	G. I. Taylor	Stability of a viscous liquid contained between two rotating cylinders. *Phil. Trans. Roy. Soc. A.*, Vol. 223, p. 289. 1923.
9	H. Görtler	Instability of laminar boundary layers on concave walls against certain three-dimensional disturbances. *Z.A.M.M.*, Vol. 21, No. 4, p. 250. 1941. (Translation A.R.C. 7658).
10	R. C. Parkhurst	N.P.L. aerofoil catalogue and bibliography. C.P. 81. July, 1951.
11	F. Cheers, W. S. Walker and C. R. Taylor.	Two-dimensional tests on a 15 per cent thick symmetrical roof-top aerofoil with 20 per cent plain flap in the N.P.L. 13 ft × 9 ft wind tunnel. R. & M. 2412. June, 1946.
12	R. W. Cumming, N. Gregory and W. S. Walker.	An investigation of the use of an auxiliary slot to re-establish laminar flow on low-drag aerofoils. R. & M. 2742. March, 1950.
13	E. Buckingham	On physically similar systems; illustrations of the use of dimensional equations. *The Physical Review*, Vol. IV, Series II, p. 345. 1914.
14	T. S. Keeble and P. B. Atkins ..	The effect of excrescences on transition; some observations in the boundary layer on Williams Glas II profile. Australian A.R.L. Aero. Note 101. May, 1951.
15	L. K. Loftin	Effects of specific types of surface roughness on boundary-layer transition. N.A.C.A. A.C.R. L5J29a. (T.I.B. 1272). February, 1946.

PART II

Brief Flight Tests on a Vampire I Aircraft to Determine the Effect of Isolated Surface Pimples on Transition

1. *Introduction.*—A method is given by Gregory and Walker in Part I for estimating the height of isolated surface excrescences that are just sufficient to cause a turbulent wedge in a laminar boundary layer. It is an empirical method based on wind-tunnel tests made at the National Physical Laboratory at wind speeds up to 200 ft/sec and aerofoils of 30-in. and 60-in. chord (maximum Reynolds number of approximately 3×10^6). To provide information at flight Reynolds numbers, two flights have been made on a *Vampire* aircraft indicating the effect of tiny paint pimples on the laminar boundary layer at a Reynolds number, based on wing chord, of 25×10^6 near sea-level.

It was found that the critical pimple height at 0·03-chord was 0·001 in. increasing to 0·003 in. at 0·20-chord, values which are within experimental error of those estimated by the method of Ref. 1. Although the pimples were of no specific shape, *e.g.*, cylindrical or conical, it is suggested that, in view of the close agreement between estimated and observed results, no further flight tests are necessary.

2. *Method of Test.*—A prepared laminar-flow region of the upper surface of the wing of *Vampire I.* TG.299 was used for the tests and surface excrescences were represented by smooth spots of paint filler ranging in size from mere specks to spots of $\frac{1}{8}$-in. in diameter. They were scattered indiscriminately with respect to size in a band about 4-in. in width running diagonally from the wing leading edge at a point where the local chord was 60 in. to a point at about 0·2-chord further inboard, where the local chord was 80 in. The spots were applied from a spray-gun working at only 1 lb/sq in. When dry the spots were convex in shape varying in diameter to height ratio from about 4 up to 56. In general the smaller spots had the larger diameter/height ratio as is shown in Fig. 1, but the accuracy of measuring such tiny pimples (using a dial gauge) is very small compared with their actual size. For instance, the accuracy of height measurement is about $\pm \frac{1}{3}$ thou. ($\pm$ 0·0003) and as the critical pimple height near the leading edge is about 1 thou. (Fig 21) it is clear that the points will show considerable scatter in this region, but this does not affect the order of the result obtained.

To indicate transition the sublimation technique was employed using acenaphthene as the volatile solid. It was sprayed as a $4\frac{1}{2}$ per cent solution in petroleum ether at 20 c.c. per sq ft.

The tests were limited to two flights and were made at an equivalent airspeed of 400 knots at an altitude of 1,000 ft ($M = 0{\cdot}62$, $C_L = 0{\cdot}06$; true speed = 690 ft/sec). Under these conditions the wing incidence would be between zero and $+\frac{1}{2}$ deg and the Reynolds number based on local chord about 25×10^6. No actual pressure plots have ever been made so close to the nose of the *Vampire* section, but there should be a favourable pressure gradient as far back as about 30 per cent chord. The local wing thickness/chord ratio is about 12 per cent located at 40 per cent with a camber of about 0·09 per cent.

3. *Results and Discussions.*—The height of pimples which caused wedges of turbulent flow and also those that had no visible effect on the laminar boundary layer are plotted against distance along the surface (in terms of percentage chord) in Fig. 21. It can be seen that near the leading edge at about $2\frac{1}{2}$ per cent chord, a pimple of about 1 thou. in height causes transition while further aft at 20 per cent chord a pimple 3 thou. high is needed. This increase in critical height further aft is consistent with the thickening of the laminar boundary layer, but clearly the order of spot or pimple height required to produce transition is very small.

Also on Fig. 21 is shown a curve of critical pimple height derived from Part I for a 13 per cent thick aerofoil at zero incidence and the agreement with the flight results is very good indeed. A further point of interest is that three points have been plotted, circumscribed by a square,

which instead of producing immediate transition at the pimple, produced two fine parallel lines extending about 1 in. downstream before spreading into a wedge. Similar lines were observed in the N.P.L. tests of Part I and were interpreted there as indicating that the pimple height was barely capable of causing a wedge to form. It is to be expected therefore that these three points should be close to the line of critical height, and bearing in mind the accuracy with which the paint pimples could be measured, the critical height line estimated from the low Reynolds number results of Part I is without doubt of the right order.

In these flight tests no attempt was made to produce pimples of particular geometric shape, but the diameter/height ratio of all the spots measured is shown against each point in Fig. 21. The estimated curve is strictly applicable to only conical and cylindrical shapes, but the fact that there is this discrepancy in geometric form does not seem to have affected appreciably the agreement with the flight tests.

4. *Conclusions.*—The height of pimple likely to cause transition, estimated by the method of Part I, agrees very well with the height determined from flight tests on a *Vampire* aircraft at a speed of about 700 ft/sec, and a Reynolds number, based on wing chord, of 25×10^6. Differences in pimple shape do not appear to affect the critical height appreciably, which is of the order of 0·001 in. near the leading edge increasing to 0·003 in. at 0·2-chord.

In view of the remarkably close agreement reached in these tests between the estimates and the flight results, no further flight tests are proposed.

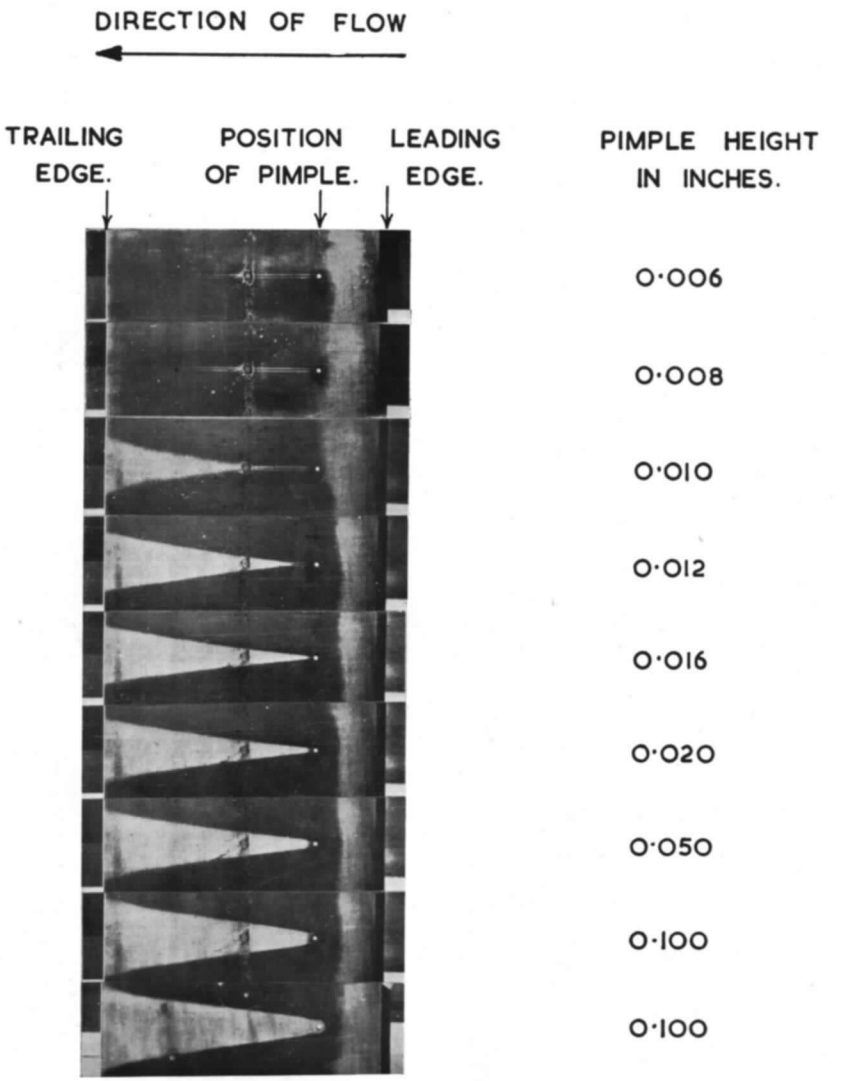

FIG. 1. Cylindrical pimples 0·2-in. diameter 0·375 ft from the leading edge. Wind speed 120 ft/sec.

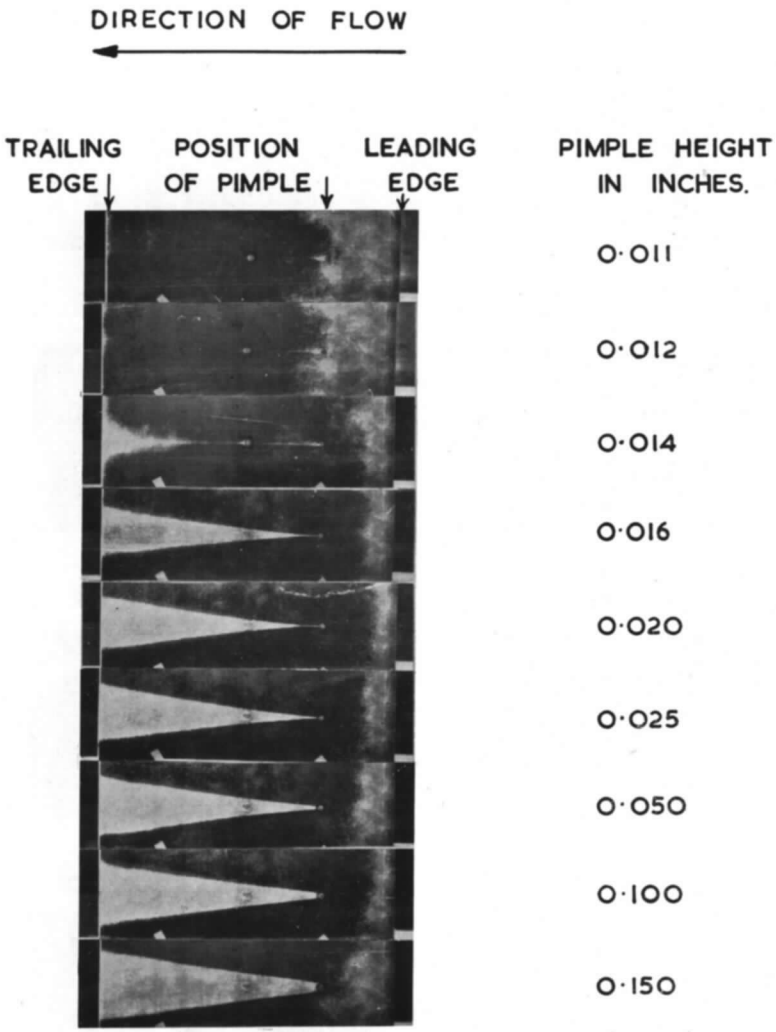

FIG. 2. Conical pimples 0·375 ft from the leading edge. Wind speed 120 ft/sec.

Turbulent wakes produced by pimples of varying height on a flat plate.

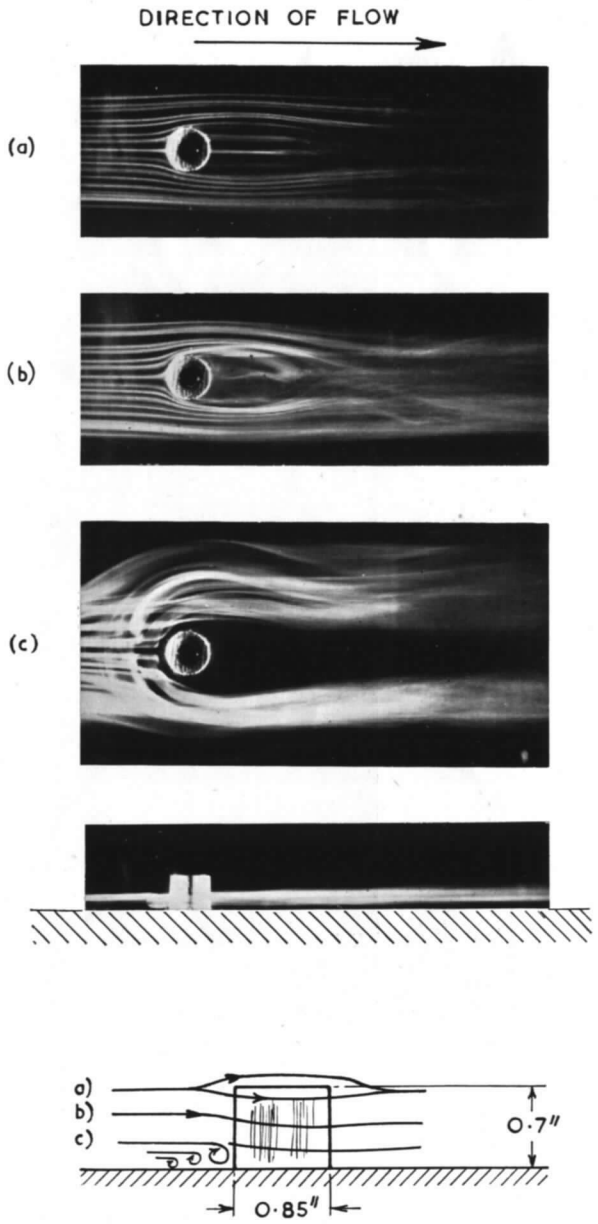

FIG. 3. Smoke flow round various sections of a cylindrical pimple in a boundary layer. Boundary-layer thickness ≏ 1 in. Wind speed ≏ 4 ft/sec.

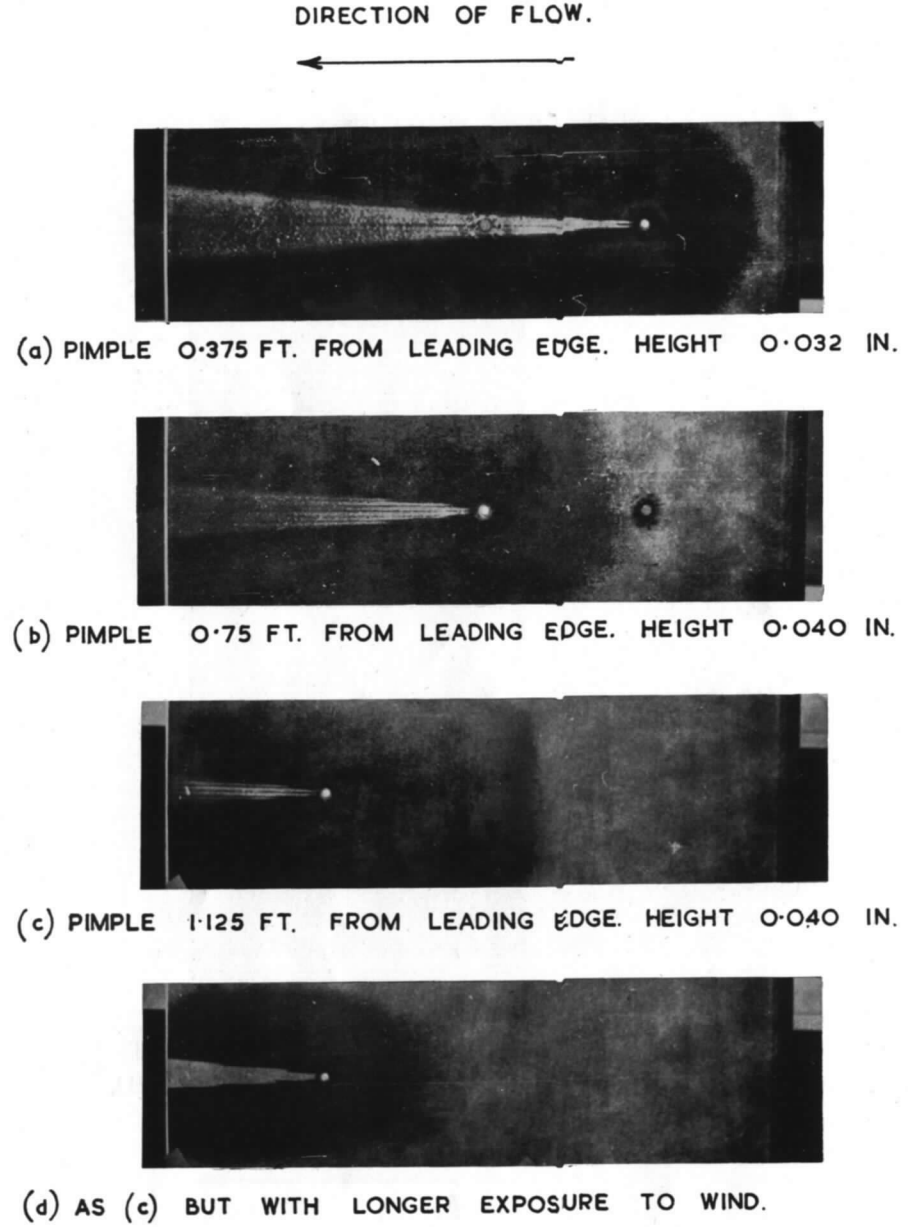

FIG. 4. Fine structure shown in turbulent wakes by china-clay technique. Cylindrical pimples 0·2-in. diameter. Wind speed 40 ft/sec.

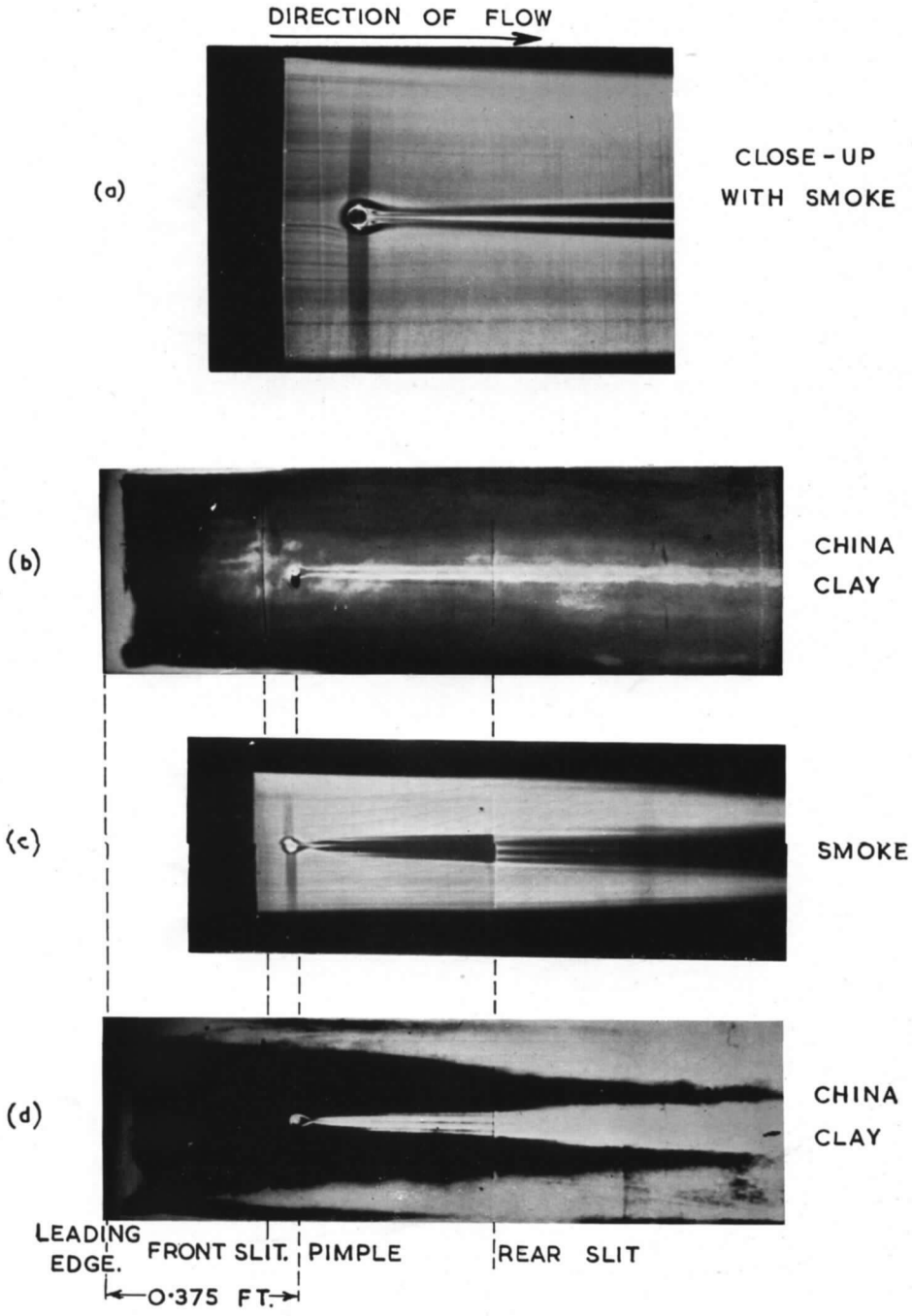

FIG. 5. Visualisation of flow past a cylindrical pimple in a boundary layer. Diameter 0·2 in. Height 0·060 in.

(a) and (b) Wind speed 8 ft/sec. Pimple height under critical.

(c) and (d) Wind speed 14 ft/sec. Pimple height equal to critical

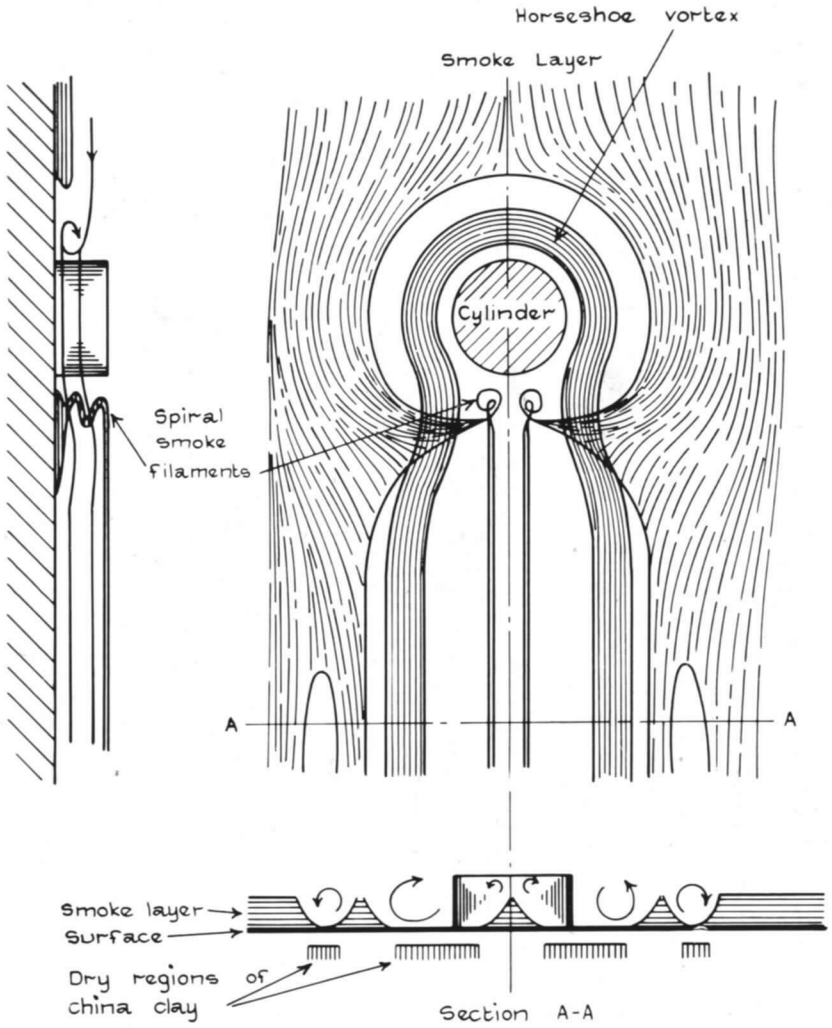

FIG. 6. Diagrammatic representation of flow past a cylindrical pimple in a boundary layer. Not to scale.

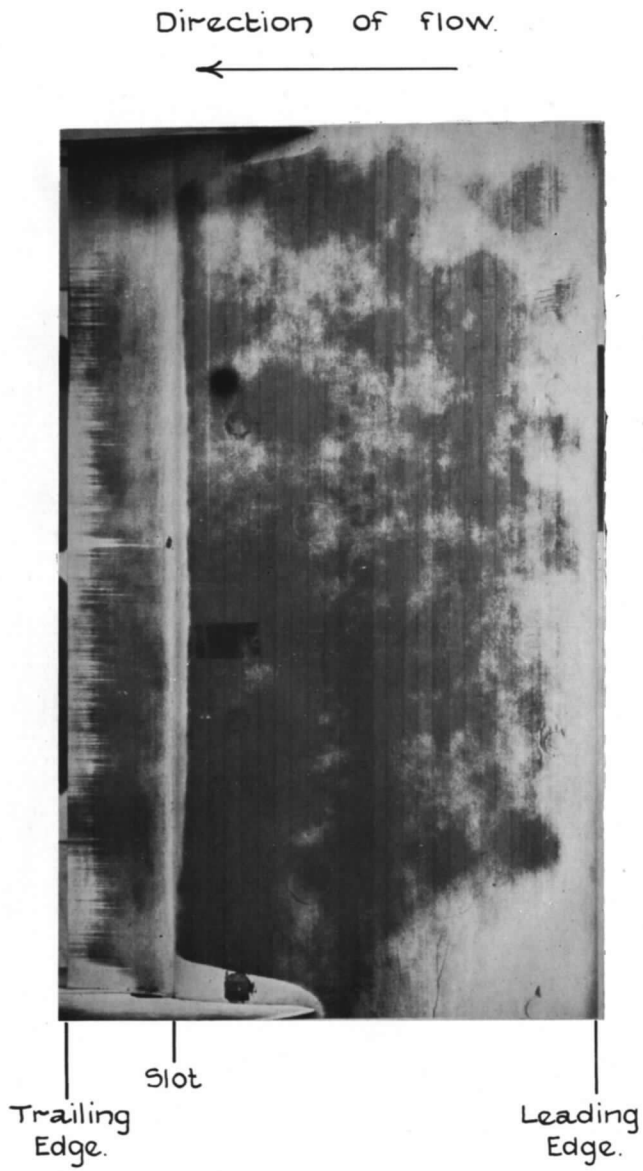

FIG. 7. Görtler vortices visualised on a concave flap surface by china-clay technique. 30 per cent Griffith aerofoil. $R = 2{\cdot}88 \times 10^6$. Complete withdrawal of boundary layer into slot ahead of flap

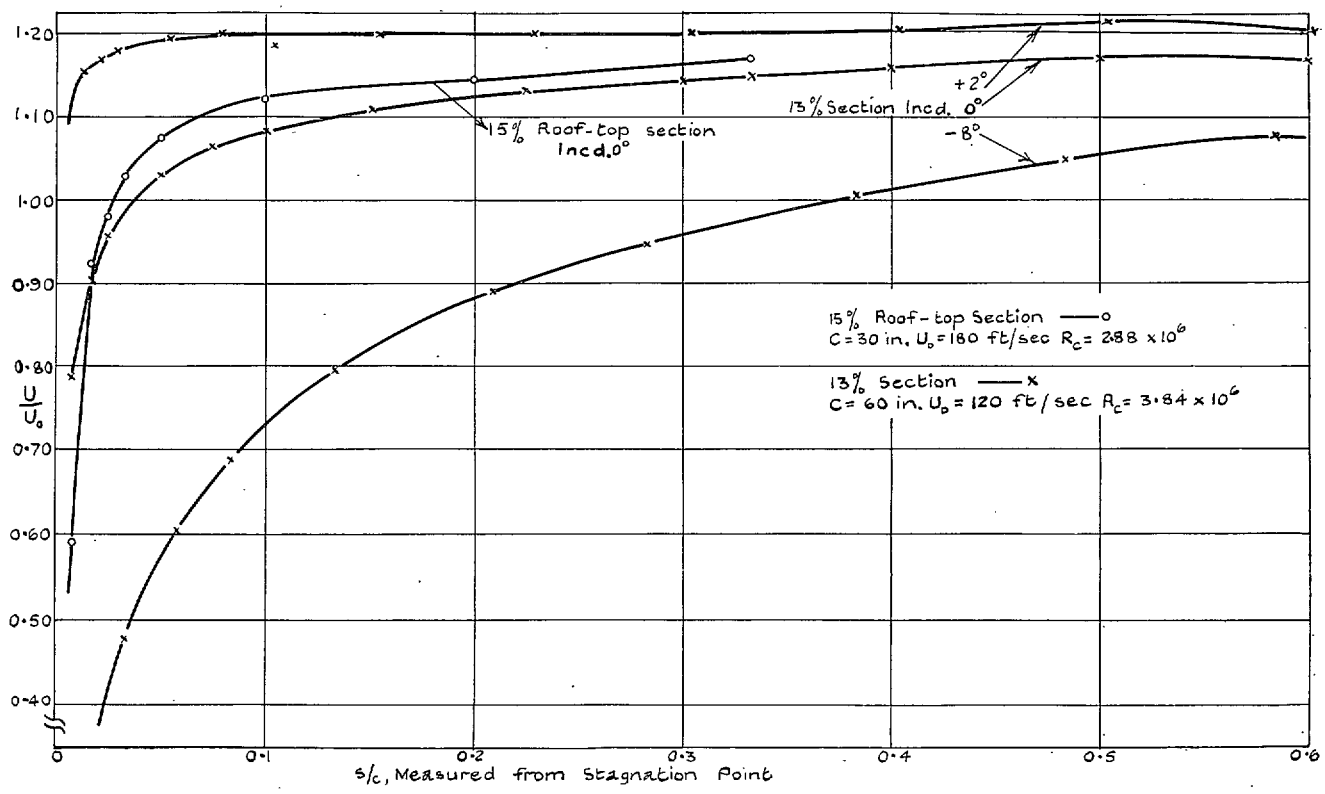

FIG. 8. Experimental velocity distributions on 13 per cent and 15 per cent sections.

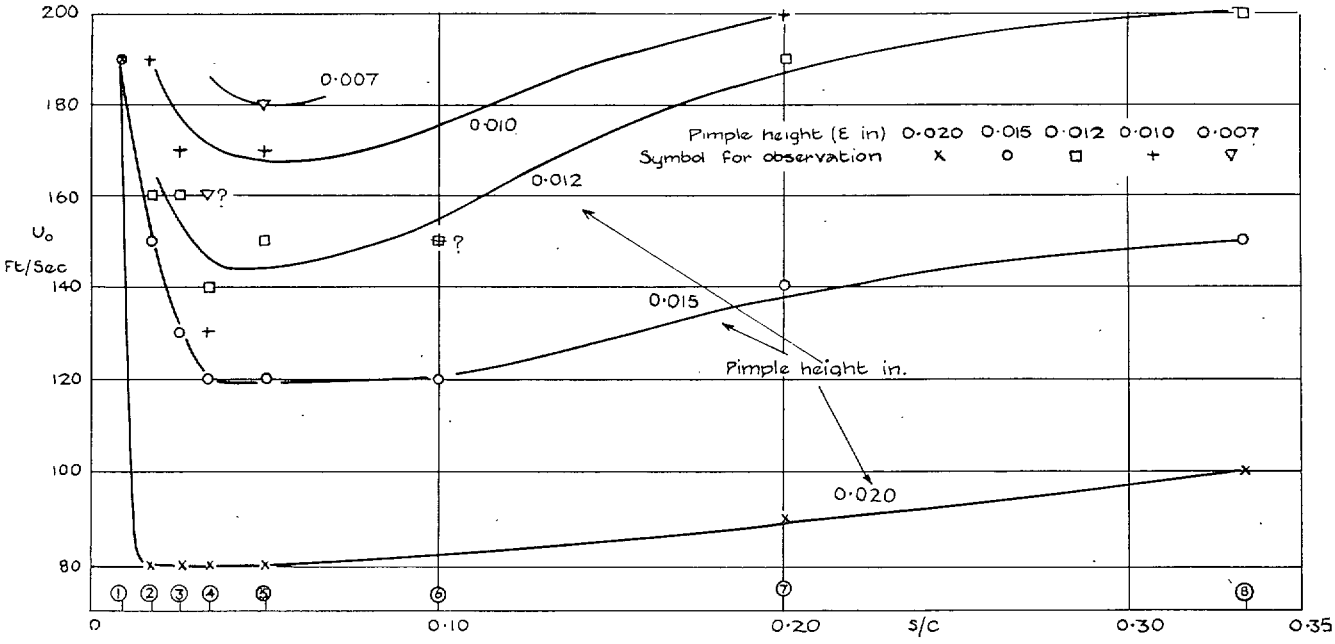

FIG. 9. Variation of critical tunnel wind speed with pimple height and position along surface.
15 per cent Roof-top section, incidence 0 deg. Cylindrical pimples.

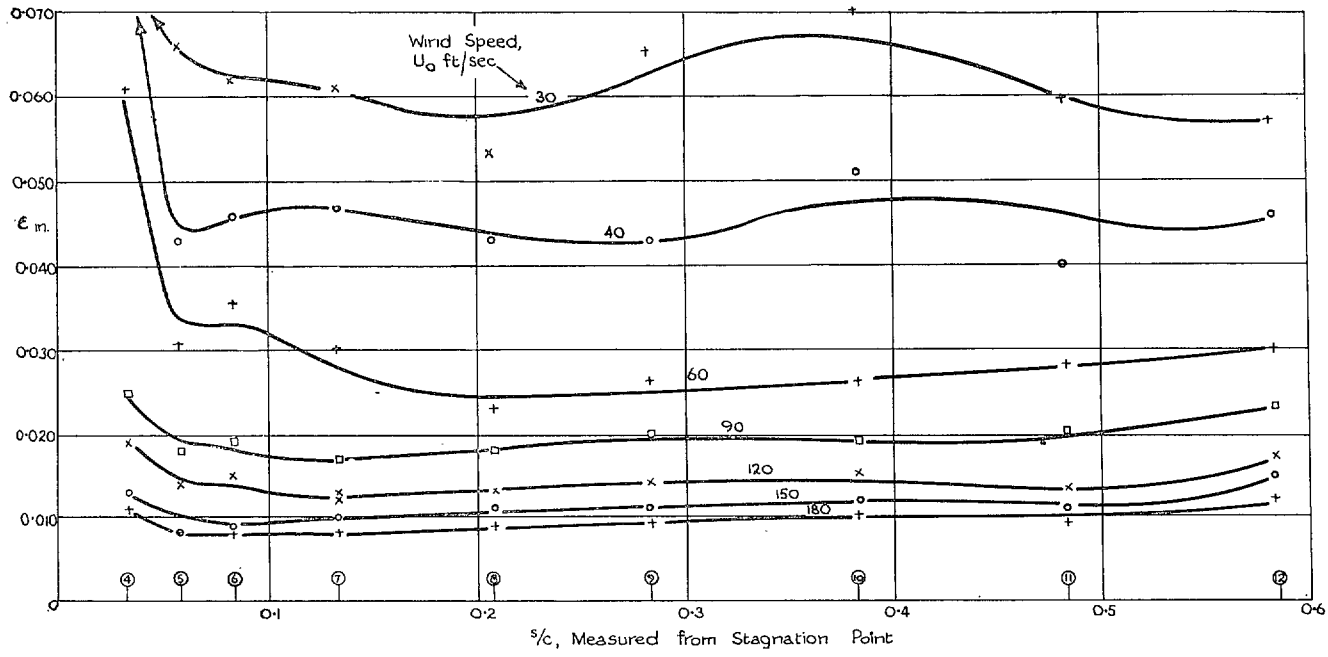

FIG. 10. Variation of critical pimple height with position along surface and tunnel-wind speed. 13 per cent aerofoil, incidence — 8 deg. Conical pimples.

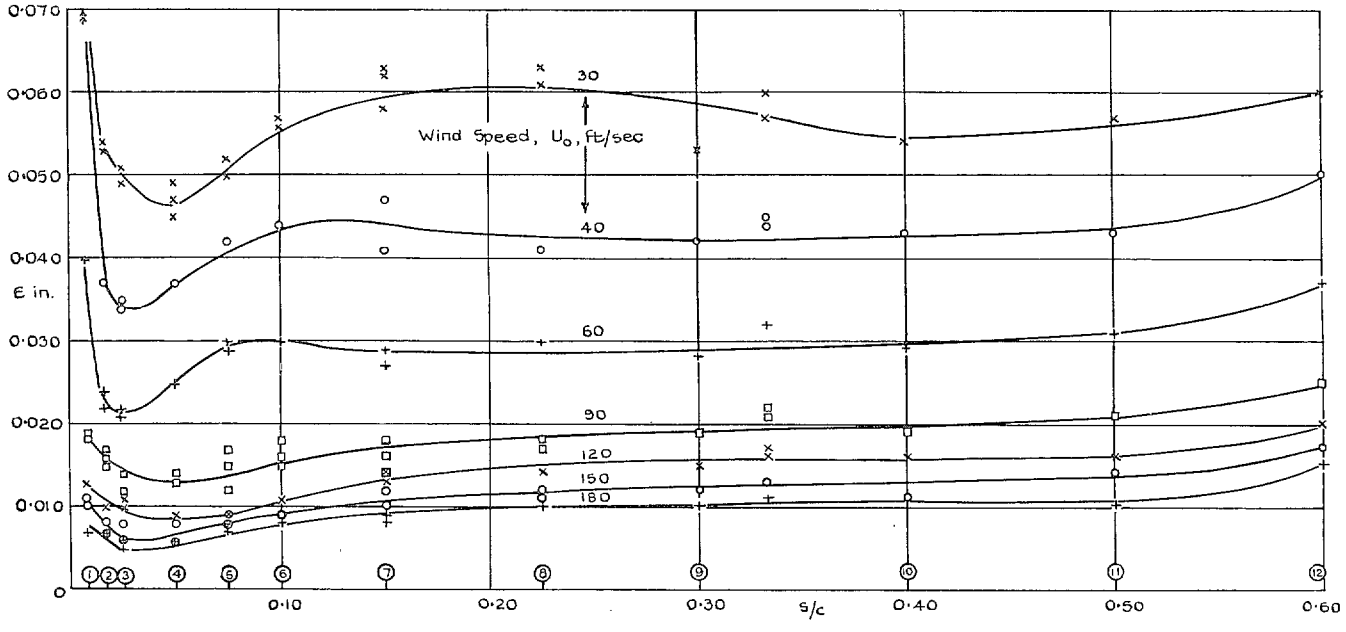

FIG. 11. Variation of critical pimple height with position along surface and tunnel-wind speed. 13 per cent aerofoil, incidence 0 deg. Conical pimples.

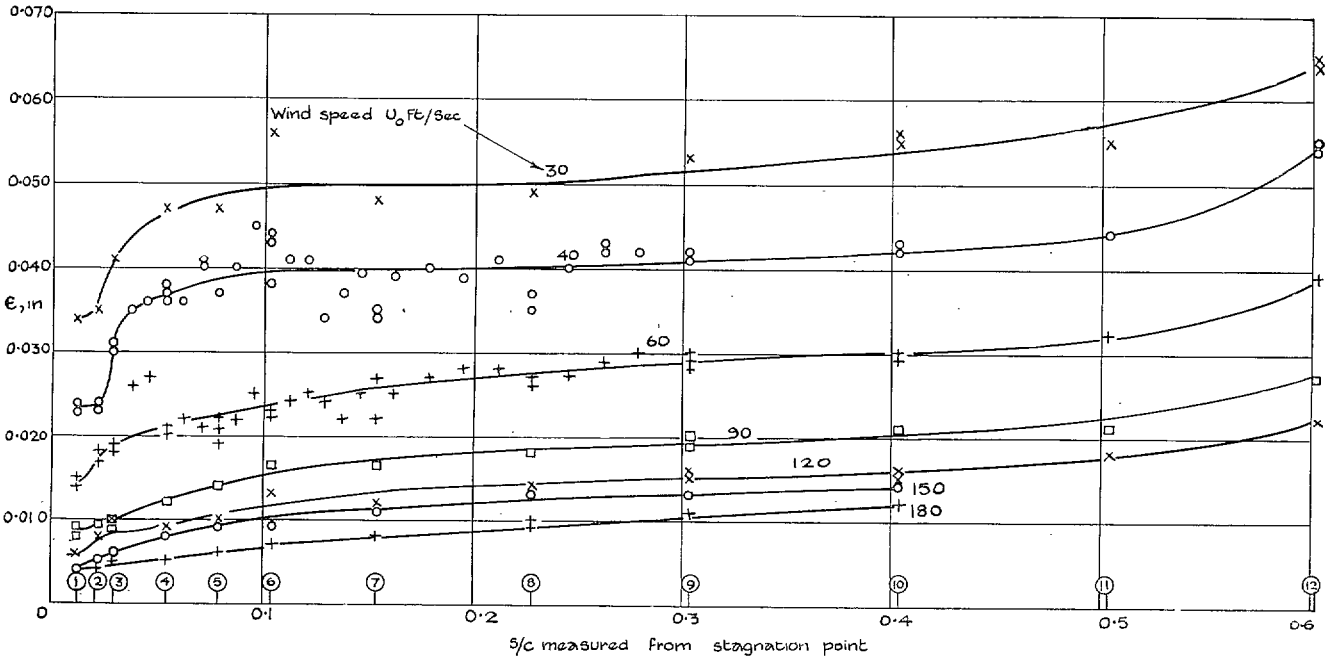

FIG. 12. Variation of critical pimple height with position along surface and tunnel-wind speed. 13 per cent aerofoil, incidence + 2 deg. Conical pimples.

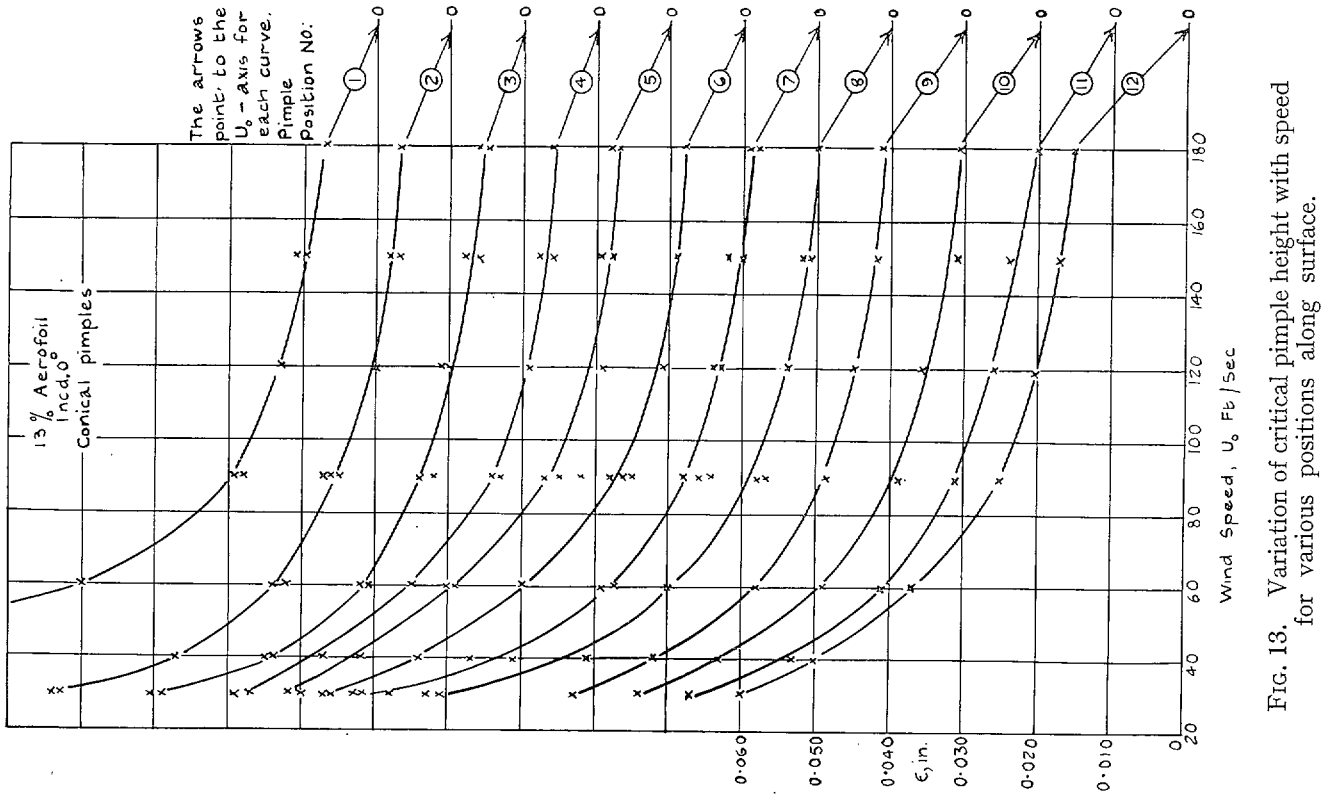

FIG. 13. Variation of critical pimple height with speed for various positions along surface.

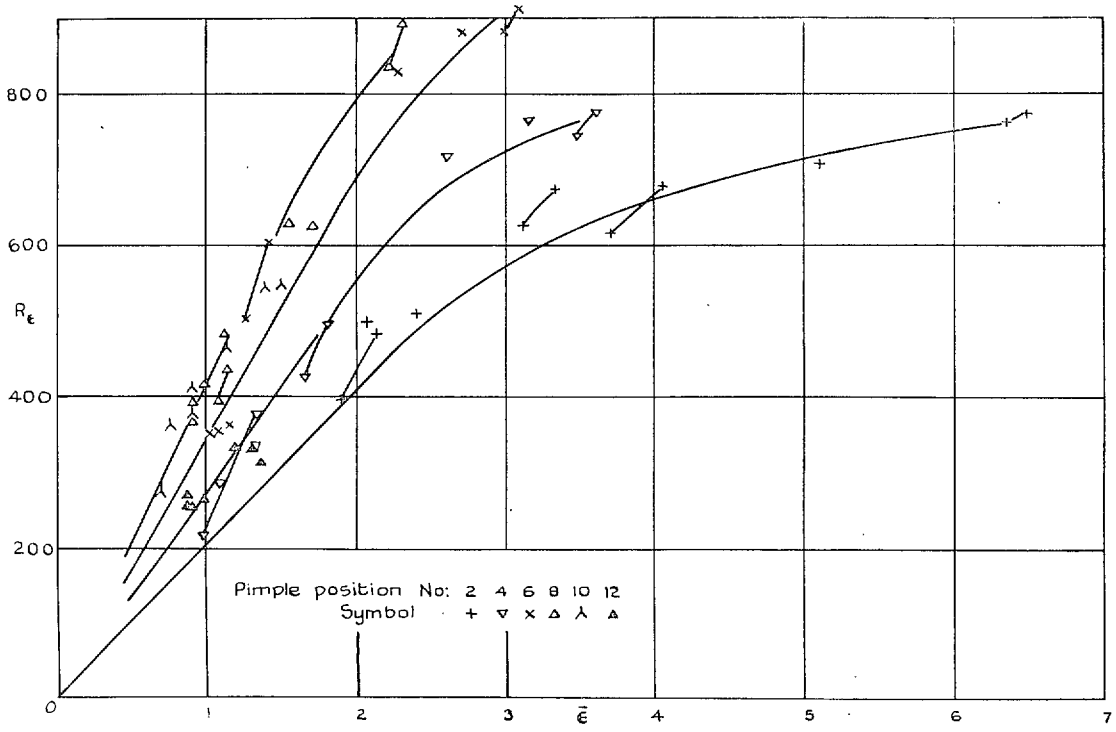

FIG. 14. Relation between R_ϵ and $\bar{\epsilon}$. 13 per cent aerofoil, incidence 0 deg.

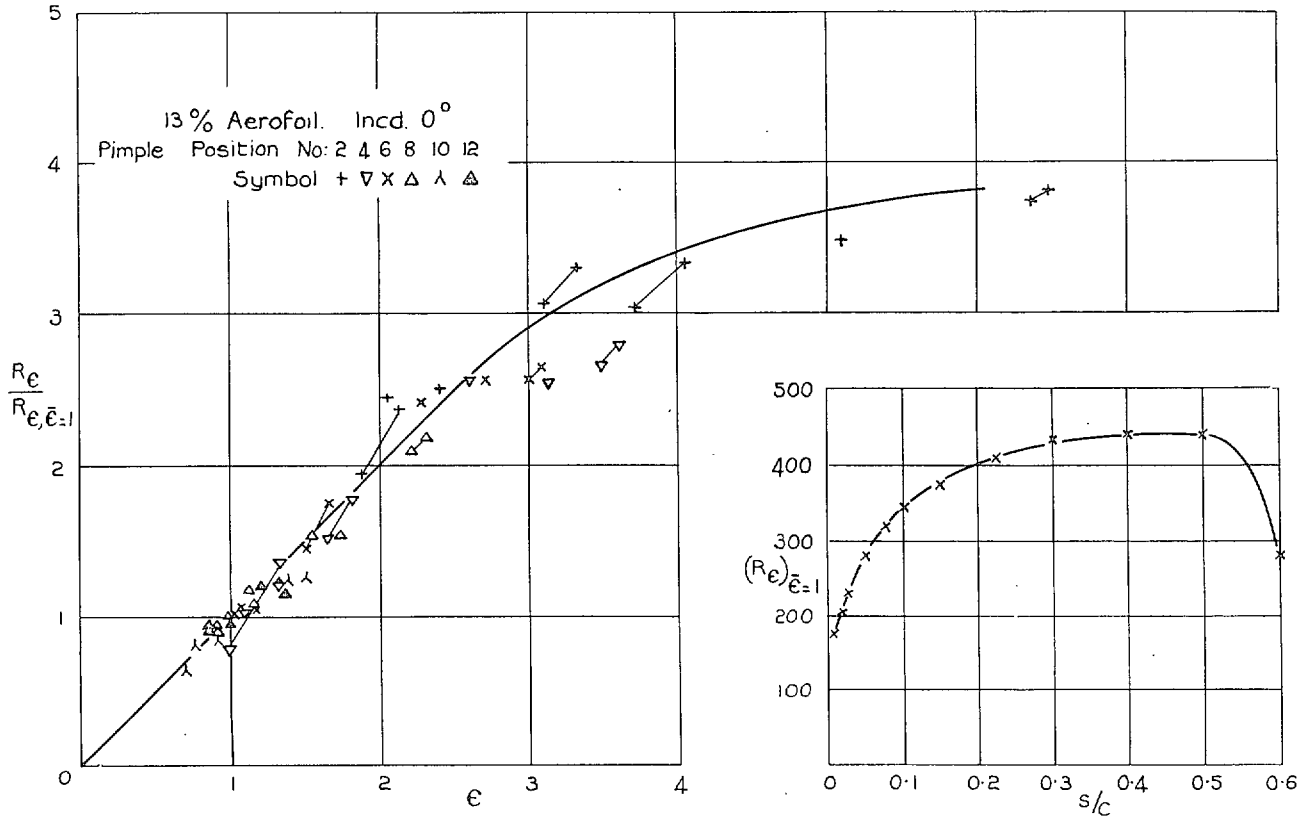

FIG. 15. 13 per cent aerofoil, incidence 0 deg.

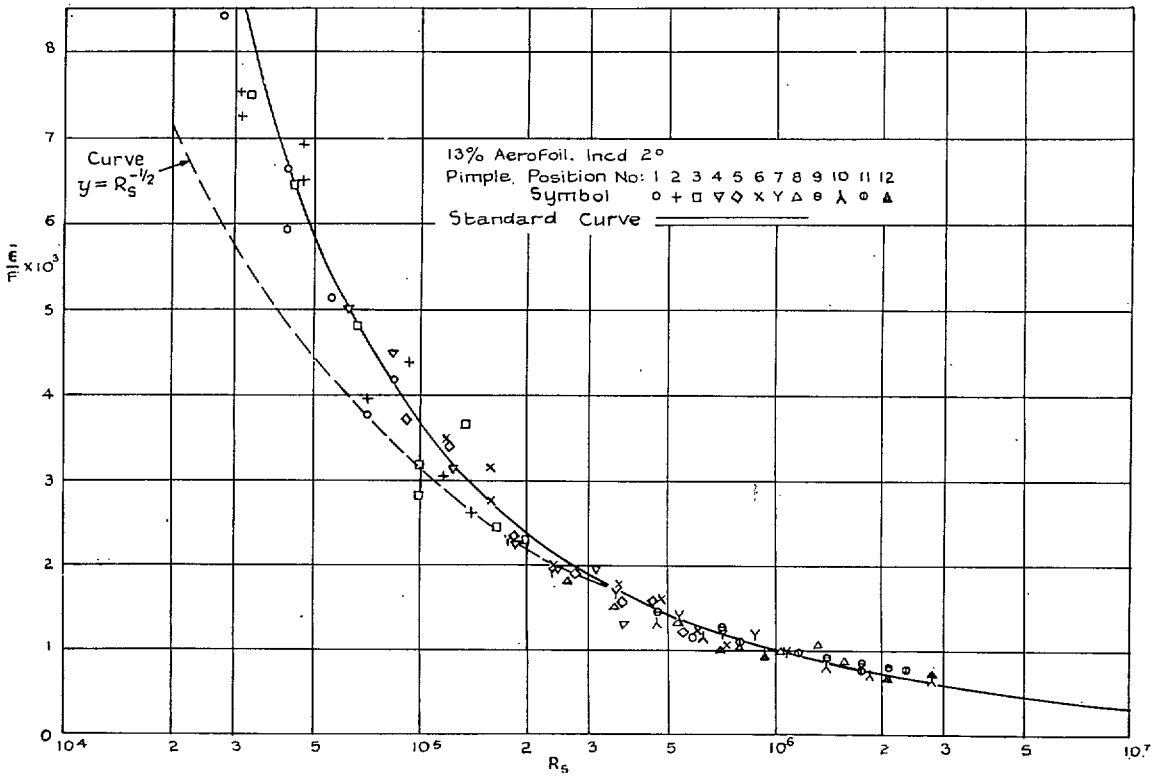

FIG. 16. 13 per cent aerofoil, incidence 2 deg.

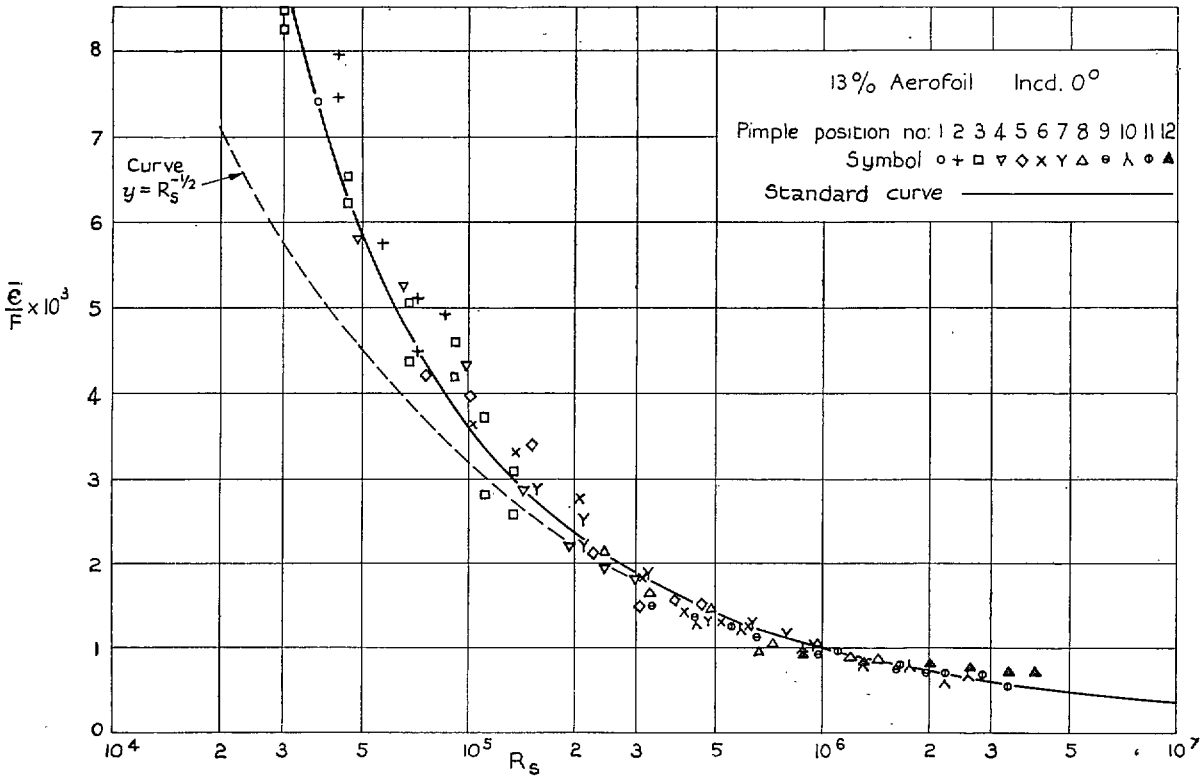

FIG. 17. 13 per cent aerofoil, incidence 0 deg.

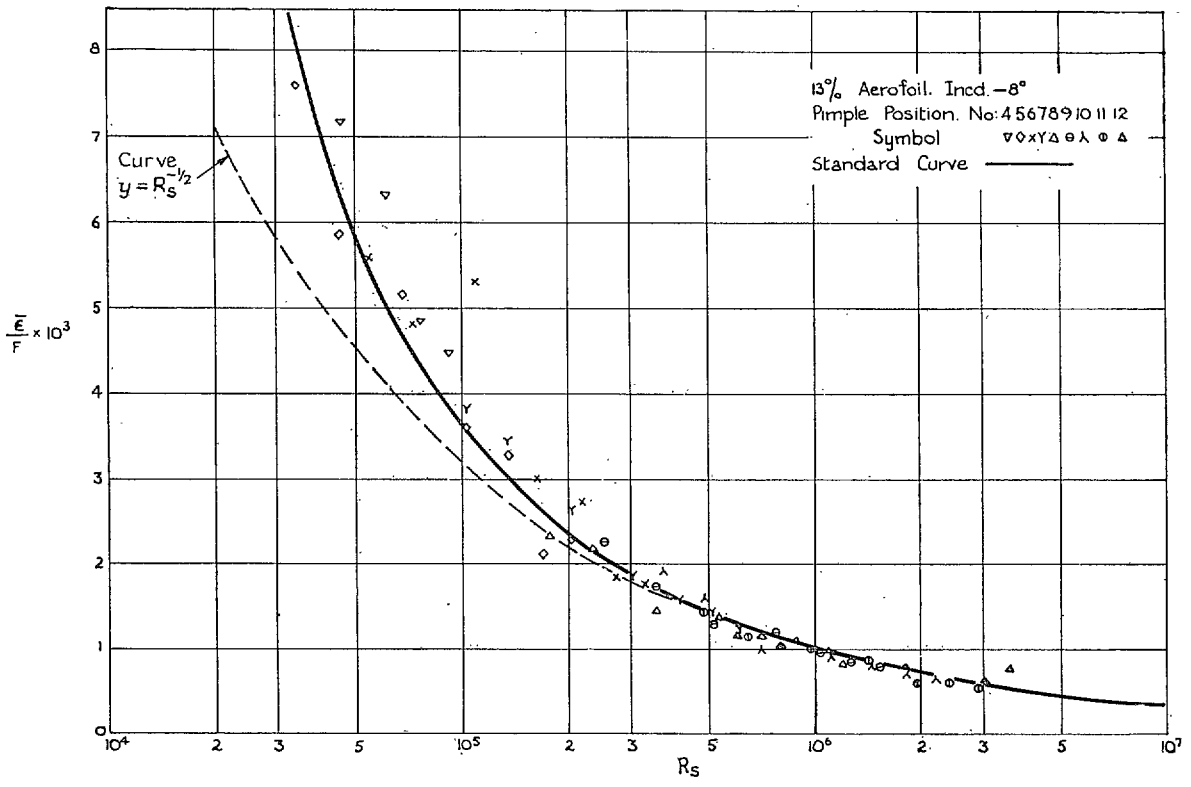

FIG. 18. 13 per cent aerofoil, incidence — 8 deg.

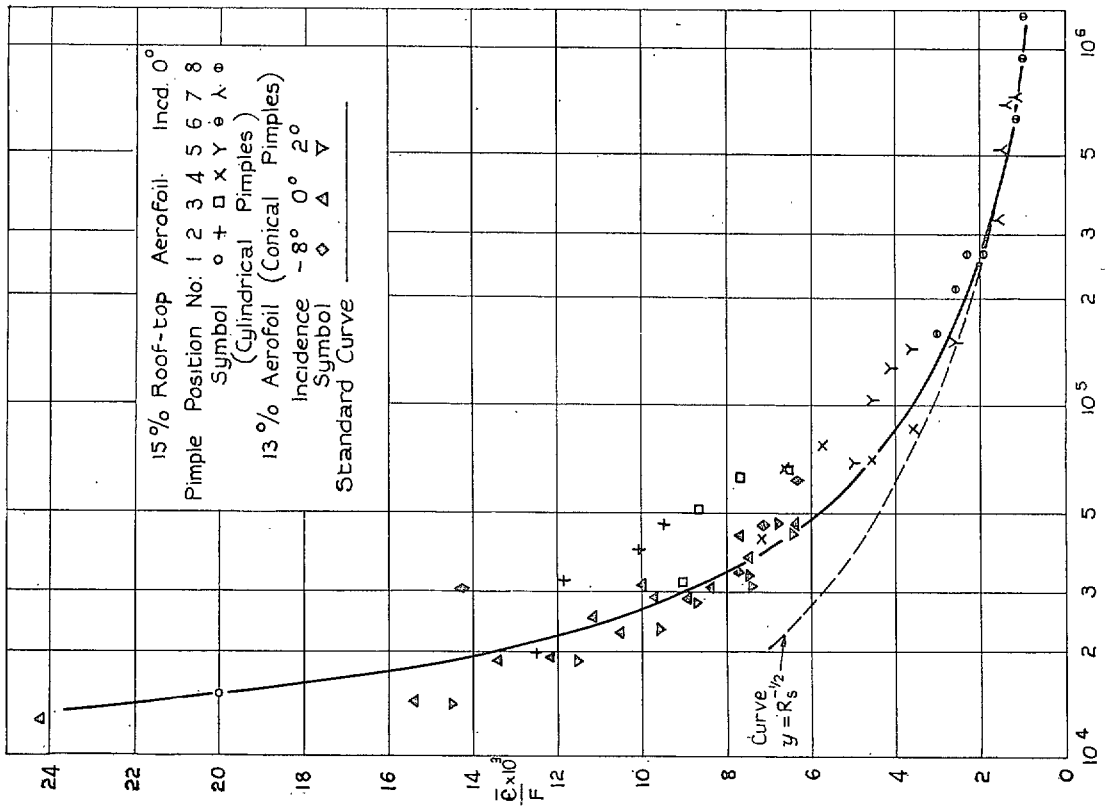

FIG. 19. 15 per cent Roof-top aerofoil, incidence 0 deg: and 13 per cent aerofoil.

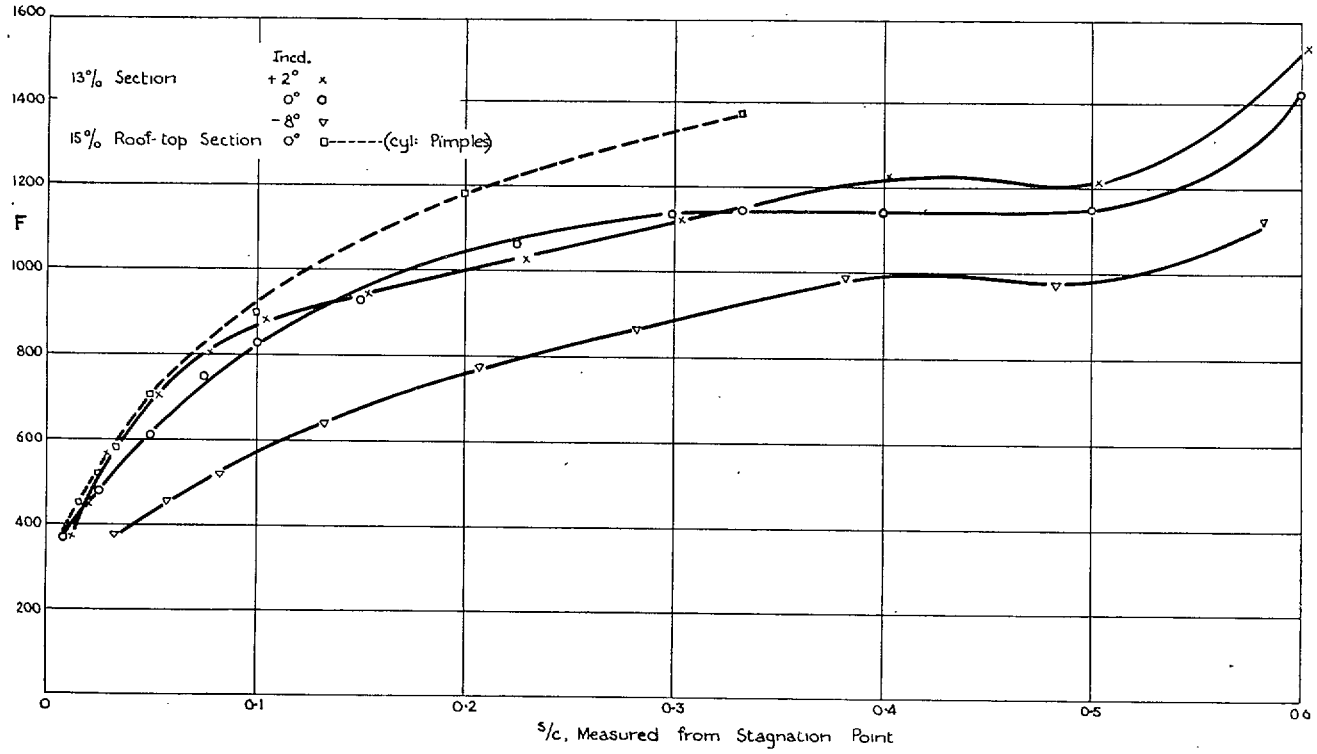

FIG. 20. Chordwise variation of F.

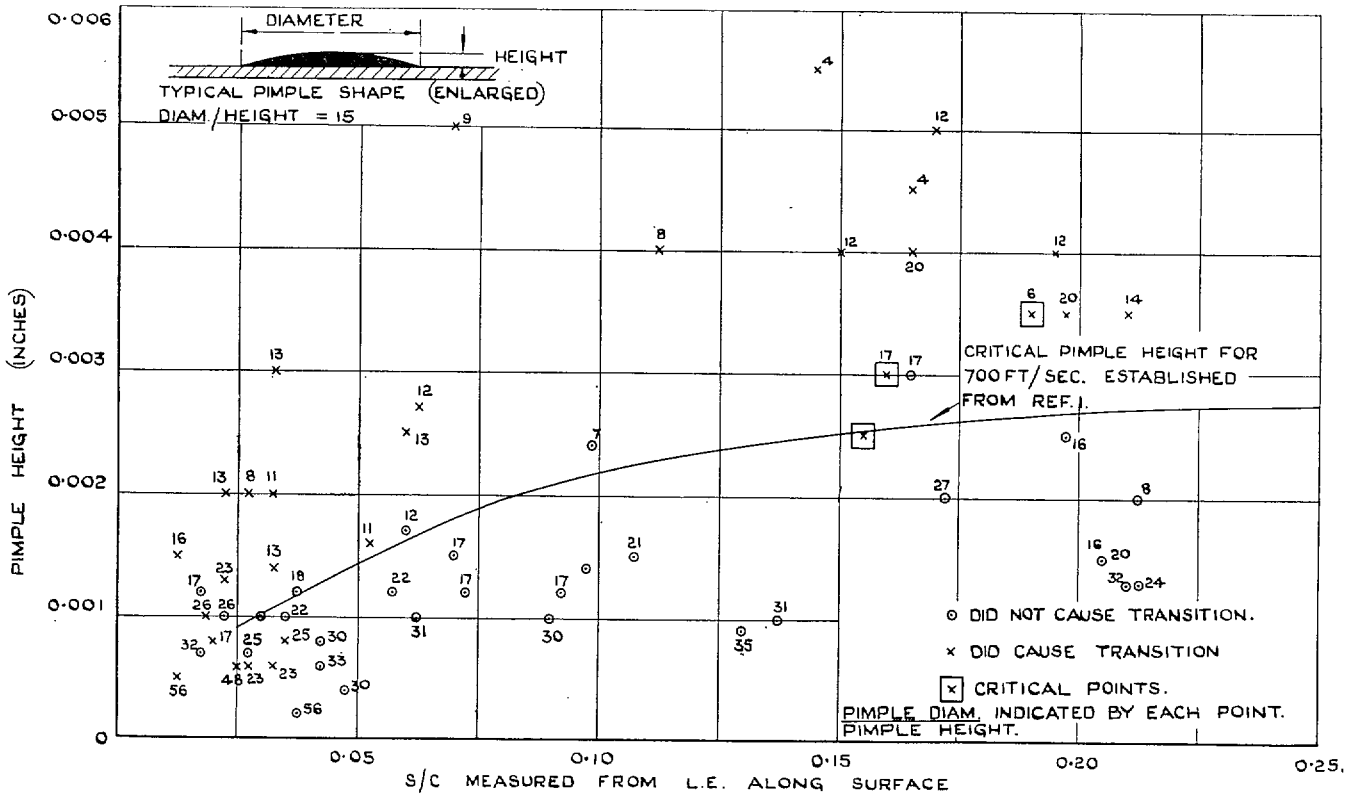

FIG. 21. *Vampire*—effect of paint pimples on transition at 400 knots.

Wt. 18/9296 K.71 2/56 G.G. 34–262

PRINTED IN GREAT BRITAIN

Publications of the Aeronautical Research Council

ANNUAL TECHNICAL REPORTS OF THE AERONAUTICAL RESEARCH COUNCIL (BOUND VOLUMES)

1939 Vol. I. Aerodynamics General, Performance, Airscrews, Engines. 50*s.* (51*s.* 9*d.*)
Vol. II. Stability and Control, Flutter and Vibration, Instruments, Structures, Seaplanes, etc. 63*s.* (64*s.* 9*d.*)

1940 Aero and Hydrodynamics, Aerofoils, Airscrews, Engines, Flutter, Icing, Stability and Control, Structures, and a miscellaneous section. 50*s.* (51*s.* 9*d.*)

1941 Aero and Hydrodynamics, Aerofoils, Airscrews, Engines, Flutter, Stability and Control Structures. 63*s.* (64*s.* 9*d.*)

1942 Vol. I. Aero and Hydrodynamics, Aerofoils, Airscrews, Engines. 75*s.* (76*s.* 9*d.*)
Vol. II. Noise, Parachutes, Stability and Control, Structures, Vibration, Wind Tunnels. 47*s.* 6*d.* (49*s.* 3*d.*)

1943 Vol. I. Aerodynamics, Aerofoils, Airscrews. 80*s.* (81*s.* 9*d.*)
Vol. II. Engines, Flutter, Materials, Parachutes, Performance, Stability and Control, Structures. 90*s.* (92*s.* 6*d.*)

1944 Vol. I. Aero and Hydrodynamics, Aerofoils, Aircraft, Airscrews, Controls. 84*s.* (86*s* 3*d.*)
Vol. II. Flutter and Vibration, Materials, Miscellaneous, Navigation, Parachutes, Performance, Plates and Panels, Stability, Structures, Test Equipment, Wind Tunnels. 84*s.* (86*s.* 3*d.*)

1945 Vol. I. Aero and Hydrodynamics, Aerofoils. 130*s.* (132*s.* 6*d.*)
Vol. II. Aircraft, Airscrews, Controls. 130*s.* (132*s.* 6*d.*)
Vol. III. Flutter and Vibration, Instruments, Miscellaneous, Parachutes, Plates and Panels, Propulsion. 130*s.* (132*s.* 3*d.*)
Vol. IV. Stability, Structures, Wind Tunnels, Wind Tunnel Technique. 130*s.* (132*s.* 3*d.*)

Annual Reports of the Aeronautical Research Council—

1937 2*s.* (2*s.* 2*d.*) 1938 1*s.* 6*d.* (1*s.* 8*d.*) 1939–48 3*s.* (3*s.* 3*d.*)

Index to all Reports and Memoranda published in the Annual Technical Reports, and separately—

April, 1950 R. & M. 2600. 2*s.* 6*d.* (2*s.* 8*d.*)

Author Index to all Reports and Memoranda of the Aeronautical Research Council—

1909–January, 1954. R. & M. No. 2570 15*s.* (15*s.* 6*d.*)

Indexes to the Technical Reports of the Aeronautical Research Council—

December 1, 1936 — June 30, 1939.	R. & M. No. 1850.	1*s.* 3*d.* (1*s.* 5*d.*)
July 1, 1939 — June 30, 1945.	R. & M. No. 1950.	1*s.* (1*s.* 2*d.*)
July 1, 1945 — June 30, 1946	R. & M. No. 2050.	1*s.* (1*s.* 2*d.*)
July 1, 1946 — December 31, 1946.	R. & M. No. 2150.	1*s.* 3*d.* (1*s.* 5*d.*)
January 1, 1947 — June 30, 1947.	R. & M. No. 2250.	1*s.* 3*d.* (1*s.* 5*d.*)

Published Reports and Memoranda of the Aeronautical Research Council—

Between Nos. 2251–2349	R. & M. No. 2350.	1*s.* 9*d.* (1*s.* 11*d.*)
Between Nos. 2351–2449	R. & M. No. 2450.	2*s.* (2*s.* 2*d.*)
Between Nos. 2451–2549	R. & M. No. 2550.	2*s.* 6*d.* (2*s.* 8*d.*)
Between Nos. 2551–2649	R. & M. No. 2650.	2*s.* 6*d.* (2*s.* 8*d.*)

Prices in brackets include postage

HER MAJESTY'S STATIONERY OFFICE

York House, Kingsway, London W.C.2; 423 Oxford Street, London W.1 (Post Orders: P.O. Box 569, London S.E.1); 13a Castle Street, Edinburgh 2; 39 King Street, Manchester 2; 2 Edmund Street, Birmingham 3; 109 St. Mary Street, Cardiff; Tower Lane, Bristol 1; 80 Chichester Street, Belfast, or through any bookseller

S.O. Code No. 23–2779